Contribution of boundness and motion of nucleons to the EMC effect

B.L. Birbrair, M.G. Ryskin and V.I. Ryazanov

Petersburg Nuclear Physics Institute

Gatchina, St. Petersburg 188300, Russia

Abstract

The kinematical corrections to the structure function of nucleon in nucleus due to the boundness and motion of nucleons arise from the excitation of the doorway states for one-nucleon transfer reactions in the deep inelastic scattering on nuclei.

1 Introduction

It is known more than 20 years that the cross section of deep inelastic scattering (DIS) on nuclear target is not equal to the sum of cross sections on free nucleons [1]. This means that the interaction inside the nucleus distorts the parton distribution in a nucleon. But at first it is necessary to single out the kinematical effects arising from the boundness and motion of nucleons in nuclei because otherwise it is hardly possible to conclude what actually happends with the nucleon structure functions in nuclear matter. This is the aim of our work rather than the explanation of the EMC effect. The above kinematical effect is due to the fact that the four-momentum of nucleon in nucleus is not equal to that of a free nucleon. Indeed, the heavy photon (γ^*) is absorbed by a single nucleon and the Deep Inelastic Scattering (DIS) proceeds via the following stage:

$$l \; + \; A \to l' \; + \; X \; + \; (A-1)^*,$$

1

where l and l' denote the incoming and outgoing leptons, X - the final hadronic state after the γ^*-nucleon interaction and A is the target nucleus. Before absorbing the heavy photon (γ^*) the struck nucleon has a certain energy-momentum distribution in nucleus. Besides this the "residual" $(A-1)$ nucleus is excited.

There were a few attempts to account for the Fermi motion, boundness and the change of the effective γ-nucleon flux factor inside the nucleus [2, 3, 4] (see [5] and references therein for more details). They all were based on a seemingly obvious assumption that the energy-momentum distribution of the struck nucleon is described by the ground-state one-nucleon spectral function.

$$S_g(\mathbf{p}, \varepsilon) = \langle A_0|a^+(\mathbf{p})\delta\Big(\varepsilon + H - \mathcal{E}_0(A)\Big)a(\mathbf{p})|A_0\rangle \ , \qquad (1)$$

where $|A_0\rangle$ is the ground state of target nucleus A, $a(\mathbf{p})$ and $a^+(\mathbf{p})$ are operators of nucleon with the momentum $\mathbf{p}$ (the spin and isospin variables are omitted), H is the nuclear Hamiltonian in the second quantization and $\mathcal{E}_0(A)$ is the ground-state binding energy of nucleus A. The calculations [3] were performed by using the following semiempirical model for the quantity (1): the nucleon energy distributions were described by the experimental data on the separation energies of protons from the $(e, e'p)$ reactions [6] (the difference between the proton and neutron separation energies was neglected leading to about 10% error) and calculating the momentum distributions within the harmonic oscillator model with the parameter $\hbar\omega_0 = (45\,A^{-1/3} - 25\,A^{-2/3})$ MeV reproducing the observed rms radii of nuclei.

However nobody realized in this connection that the DIS on nuclei is rapid process, and therefore the energy-momentum distribution of struck nucleon is described by the spectral function of nuclear mode which is excited via a sudden perturbation rather than that of the ground state. Our work is based on the fact that the relevant mode is provided by the doorway states for the one-nucleon transfer reactions. As demonstrated in [7]–[9] the above states are eigenstates of nucleon in the static nuclear field.

Recall that the microscopic nuclear models are based on certain approximations for the in-medium nucleon mass operator M. For instance the nuclear shell model potential is the approximation for the mass operator at nuclear Fermi-surface, the optical model potential is dealing with the mass operator at low and intermediate energies, etc. In all the available approaches

the mass operator includes all the Feynman diagrams which are irreducible in the one-particle channel, and therefore it cannot be calculated. Instead it is described by a set of phenomenological parameters.

In contrast to the above models the nuclear static potential is the mass operator at the infinite value of the energy variable. Only the Hartree diagrams with the free space (*i.e.* vacuum) nuclear forces survive in this case thus permitting the model-independent calculation of the static field. So the doorway states (DS) under consideration appear to be the unique nuclear object, both model-independent and described by the exactly soluble problem.

The calculation [8] showed that the rms radii of the DS density distributions are appreciably less than those of the ground-state ones: for instance, the value of $\langle r^2 \rangle = A^{-1} \int \rho(r) r^2 d^3 r$ is $10.88\,\text{fm}^2$ for the ground state of ^{40}Ca being only $8.76\,\text{fm}^2$ for the DS. As a result the nucleon motion (*i.e.* the value of $\langle \mathbf{p}^2 \rangle$) was underestimated in [3] by about 25% [1].

In Sec. 2 we briefly describe the formalism of the DS. In Sec. 3 the DIS structure functions F_2 are calculated for different nuclei and deuteron; to single out the boundness and motion effects we disregarded the possible changes of the parton distribution inside the nucleon in nucleus. In the last Sec. 4 we compare the calculated ratios $2F_{2A}/AF_{2D}$ with the available experiments.

2 Doorway states for one-nucleon transfer reactions

2.1 Theory

Evolution of the state arising from the one-nucleon transfer to the nuclear ground state $|A_0\rangle$ at the initial time moment $t = 0$ is described by the single-particle propagator [11]

$$S(x, x'; \tau) = -i\langle A_0|T\psi(x,\tau)\psi^\dagger(x',0)|A_0\rangle =$$

---

[1] By the same reason the kinematical effect was underestimated in Ref.[10] as well.

$$= \quad i\theta(-\tau) \sum_j^{(A-1)} \Psi_j(x)\Psi_j^\dagger(x')e^{-iE_j\tau} - i\theta(\tau) \sum_k^{(A+1)} \Psi_k(x)\Psi_k^\dagger(x')e^{-iE_k\tau}. \quad (2)$$

At $\tau < 0$ it describes the evolution of the hole state,

$$\Psi_j(x) = \langle (A-1)_j|\psi(x)|A_0\rangle , \quad E_j = \mathcal{E}_0(A) - \mathcal{E}_j(A-1) , \quad (3)$$

when the nucleon is removed from the ground state A_0, whereas at $\tau > 0$ the evolution of the particle state is described,

$$\Psi_k(x) = \langle A_0|\psi(x)|(A+1)_k\rangle , \quad E_k = \mathcal{E}_k(A+1) - \mathcal{E}_0(A) , \quad (4)$$

when nucleon is added to the ground state A_0. The quantities $\mathcal{E}_j(A-1)$, $\mathcal{E}_k(A+1)$ and $\mathcal{E}_0(A)$ are total binding energies of the states $|(A-1)_j\rangle$ of the $(A-1)$ nucleus, the states $|(A+1)_k\rangle$ of the $(A+1)$ nucleus and the ground state $|A_0\rangle$ of the A one.

The Fourier transform of the propagator

$$G(x,x';\varepsilon) = \int S(x,x';\tau)e^{i\varepsilon\tau}d\tau = \sum_j^{(A-1)} \frac{\Psi_j(x)\Psi_j^\dagger(x')}{\varepsilon - E_j - i\delta} + \sum_k^{(A+1)} \frac{\Psi_k(x)\Psi_k^\dagger(x')}{\varepsilon - E_k + i\delta} ,$$
$$(5)$$
$$\delta \to +0$$

obeys the Dyson equation

$$\varepsilon G(x,x';\varepsilon) = \delta(x-x') + \hat{k}_x G(x,x';\varepsilon) + \int M(x,x_1;\varepsilon)G(x_1,x';\varepsilon)dx_1 , \quad (6)$$

where $\hat{k}_x$ is the kinetic energy and the mass operator $M(x,x';\varepsilon)$ includes all Feynman diagrams which are irreducible in the one-particle channel.

We are interested in the very beginning of the evolution, i.e. the $\tau \to 0$ limit. According to the time-energy Heisenberg relation this is equivalent to the limit $\varepsilon \to \infty$. In this limit

$$G(x,x';\varepsilon) = \frac{I_0(x,x')}{\varepsilon} + \frac{I_1(x,x')}{\varepsilon^2} + \frac{I_2(x,x')}{\varepsilon^3} + \cdots , \quad (7)$$

where (see the definition (1) of the propagator)

$$I_0(x,x') = \sum_j^{(A-1)} \Psi_j(x)\Psi_j^\dagger(x') + \sum_k^{(A+1)} \Psi_k(x)\Psi_k^\dagger(x') = i\Big[S(x,x';+0) - S(x,x';-0)\Big];$$
$$(8)$$

4

$$
\begin{aligned}
I_1(x, x') \quad &= \quad \overset{(A-1)}{\underset{j}{\sum}} E_j \Psi_j(x) \Psi_j^\dagger(x') + \overset{(A+1)}{\underset{k}{\sum}} E_k \Psi_k(x) \Psi_k^\dagger(x') \quad = \\
&= \quad -\Big[\dot{S}(x, x'; +0) - \dot{S}(x, x'; -0) \Big];
\end{aligned}
\tag{9}
$$

$$
\begin{aligned}
I_2(x, x') \quad &= \quad \overset{(A-1)}{\underset{j}{\sum}} E_j^2 \Psi_j(x) \Psi_j^\dagger(x') + \overset{(A+1)}{\underset{k}{\sum}} E_k^2 \Psi_k(x) \Psi_k^\dagger(x') \quad = \\
&= \quad -i\Big[\ddot{S}(x, x'; +0) - \ddot{S}(x, x'; -0) \Big]
\end{aligned}
\tag{10}
$$

the quantities I_0, I_1 and I_2 thus describing the very beginning of the evolution $\left(\dot{S} = \frac{\partial S}{\partial \tau}, \ddot{S} = \frac{\partial^2 S}{\partial \tau^2} \right)$.

Now consider the mass operator $M(x, x'; \varepsilon)$. It includes the energy-independent Hartree diagrams $U_{st}(x)\delta(x - x')$ (which were shown in Fig.3 of Ref.[9]) the higher-order diagrams describing the nuclear correlation effects (the lowest-order diagram of such kind was shown in Fig.4a of Ref.[9]) and the Fock ones (Fig. 4b of Ref.[9]). The correlation diagrams include the propagators of intermediate states thus behaving as ε^{-1} in the $\varepsilon \to \infty$ limit (see Ref.[12] for more stringent demonstration). The same is valid for the Fock diagrams. Indeed, the interaction between baryons proceeds via the exchange by some particles (they are quark–antiquark pairs and/or gluons in the QCD) and therefore both the momentum and the energy are transferred through the interaction. As a result the Fock diagrams also include the intermediate state propagators thus being of order of ε^{-1} in the $\varepsilon \to \infty$ limit. (In Ref. [7] this is demonstrated for the meson-nucleon intermediate state). So the mass operator in this limit is

$$
M(x, x'; \varepsilon) \ = \ U_{st}(x)\delta(x - x') + \frac{\Pi(x, x')}{\varepsilon} \ + \ \cdots
\tag{11}
$$
$$
\varepsilon \to \infty
$$

Introducing the static Hamiltonian

$$
h_{st} \ = \ \hat{k}_x + U_{st}(x)
\tag{12}
$$

let us write down the high-energy limit Dyson equation in the form

$$
\varepsilon G(x, x'; \varepsilon) = \delta(x - x') + h_{st} G(x, x'; \varepsilon) + \int \left(\frac{\Pi(x, x_1)}{\varepsilon} + \cdots \right) G(x_1, x'; \varepsilon) dx_1 \ .
\tag{13}
$$

Putting into (13) the asymptotics (7) and equating coefficients at the same powers of ε^{-1} we get

$$\sum_j^{(A-1)} \Psi_j(x)\Psi_j^\dagger(x') + \sum_k^{(A+1)} \Psi_k(x)\Psi_k^\dagger(x') \;=\; \delta(x-x') \tag{14}$$

$$\sum_j^{(A-1)} E_j\Psi_j(x)\Psi_j^\dagger(x') + \sum_k^{(A+1)} E_k\Psi_k(x)\Psi_k^\dagger(x') \;=\; h_{st}\delta(x-x') \tag{15}$$

$$\sum_j^{(A-1)} E_j^2\Psi_j(x)\Psi_j^\dagger(x') + \sum_k^{(A+1)} E_k^2\Psi_k(x)\Psi_k^\dagger(x') \;=\; h_{st}^2\delta(x-x') + \Pi(x,x'). \tag{16}$$

Equations (9), (12) and (15) may be written as

$$-\left[\dot{S}(x,x';+0) - \dot{S}(x,x';-0)\right] \;=\; h_{st}\delta(x-x') \;=\; \left[k_x + U_{st}(x)\right]\delta(x-x') . \tag{17}$$

As follows from the lhs of (17) the hamiltonian h_{st} describes the very beginning of the one-nucleon transfer process the eigenstates of h_{st} thus being the doorway states for one-nucleon transfer reactions. On the other hand the rhs of (17) shows that the hamiltonian h_{st} describes the motion of nucleon in nuclear static field $U_{st}(x)$. Indeed, the latter is expressed through the free-space NN forces rather than the effective ones thus being the nucleon field rather than the quasiparticle one. So we proved that the doorway states for one-nucleon transfer fast reactions are the eigenstates of nucleon in nuclear static field.

2.2   Doorway eigenfunctions

Since the doorway states (DS) describe the motion of the nucleon in nuclear *static* field the corresponding eigenfunctions may be calculated in a model independent way. Indeed, the two-particle forces are determined from the experimental data on the elastic nucleon-nucleon scattering (i.e. from the phase shifts analysis)[13] and the deuteron properties. The necessary information about the multiparticle forces is obtained from the observed energy spectra of the doorway states [7]. So the only additional information needed for calculation of the static field in a given nucleus is that on the nucleon density distributions in this nucleus. In all the nuclei which are treated in

the present paper these distributions are spherically symmetric thus leading to the static field with the same symmetry. Hence the quantum mechanical problem is the motion of a particle in a central field. This problem is solved with any desired accuracy and without any simplifications.

We have to emphasize that the doorway states are not the eigenfunctions of the total nuclear Hamiltonian thus being fragmented over the actual nuclear states owing to the correlation effects. The observed spreading width of the DS is about 20 MeV; that is the relaxation time $\sim 0.3 \cdot 10^{-22}$ sec. This is much larger than the time chracteristic for DIS which is of the order of $2q_0/Q^2 \simeq 1/mx \sim 3 \cdot 10^{-24}$ sec in the nucleus rest frame. So during the DIS process the DS do not have time to be distorted by the correlations thus permitting the exact account for the nucleon boundness and motion to the EMC effect.

The relevant energy-momentum distribution of nucleons for DIS is determined by the spectral function of the DS (rather than the ground state one):

$$S_{DS}(\varepsilon, \vec{p}) = S_p(\varepsilon, \vec{p}) + S_n(\varepsilon, \vec{p}) , \qquad (18)$$

where the proton spectral function is

$$S_p(\varepsilon, \vec{p}) = \frac{1}{4\pi} \sum_{\lambda}^{(p)} \nu_\lambda f_\lambda(\vec{p}) \delta(\varepsilon - \varepsilon_\lambda) . \qquad (19)$$

The sum in the r.h.s. runs over the proton DS, λ stands for the angular momentum j and other quantum numbers of a particle state in central field, ν_λ equal to $2j + 1$ for the filled states and the actual number of nucleons on partly filled ones, ε_λ are the DS energies and $f_\lambda(p)$ are found by solving the Dirac equation (see Ref.s[7, 9] for details).

$$h_{st}\psi_\lambda(\vec{r}) = \varepsilon_\lambda \psi_\lambda(\vec{r}) . \qquad (20)$$

The function $f_\lambda(p) = u_\lambda^2(p) + w_\lambda^2(p)$, given by the sum of the upper and lower components square of the bi-spinor $\psi_\lambda(p)$ (in momentum space), is normalized by the condition

$$\int f_\lambda(p)p^2 dp = 1 . \qquad (21)$$

The neutron spectral function obeys the same relation in which the proton DS are substituted by the neutron ones.

It is instructive to mention that the spectral functions $S_{DS}(\varepsilon, \vec{p})$ is evident Lorentz invariant obeying the following normalization:

$$\int S_{DS}(\varepsilon, \vec{p})d\varepsilon d^3p \ = \ \int S_{DS}(p)d^4p \ = \ A \qquad (22)$$

(here $p_0 = m + \varepsilon$, so $dp_0 = d\varepsilon$).

The calculations were performed for ^{12}C, ^{14}N, ^{27}Al, ^{40}Ca, ^{56}Fe and ^{63}Cu. The reason is as follows. As mentioned above the necessary information for the calculations is that about the proton and neutron density distributions. The former is available for throughout the whole periodic system[14], but it is not the case for the latter: the neutron densities are available only for doubly closed-shell nuclei ^{16}O, ^{40}Ca, ^{90}Zr and ^{208}Pb[15]. That's why we confined ourselves by nuclei with a small neutron excess: the density distributions per nucleon are nearly the same for protons and neutrons in these nuclei[16].

To calculate the eigen functions the Bonn B [13] and OSBEP[17] NN-potentials were used [2]. In both cases the results are very close to each other. The difference never exceeds 0.5% for $x < 0.6$ and is less then the experimental error bars in the domain where the ratio (25) $R_{th} > 1$.

3   Deep inelastic cross section on nuclear target

The DIS cross section is usually written in terms of the structure function $F_2(x, Q^2)$, that is the cross section of electron-nucleon interaction

$$\frac{d\sigma}{dxdQ^2} \simeq \frac{4\pi\alpha^2}{xQ^4}\left((1 - y + \frac{y^2}{2})F_2(x, Q^2) - \frac{y^2}{2}F_L(x, Q^2)\right) \qquad (23)$$

---

[2]For the deuteron the Bonn B wave function was used in both cases.

where we neglect the nucleon mass $m_N^2 = m^2$ in comparison with the total energy square $s = (k+p)^2 >> m^2$. Here: k, q, p are the 4-momenta of the incoming electron, heavy photon and the target nucleon repectively. $Q^2 = -q^2$, $x = Q^2/2(p \cdot q)$ and $y = (q \cdot p)/(k \cdot p)$. $\alpha = 1/137$ is the electromagnetic coupling.

As a rule the data are taken at rather small y, where the coefficient $y^2/2$ in front of the longitudinal part (F_L) is small. Next, the ratio $R^L = F_L/F_2 \sim 0.2$ is not large. Moreover, unlike the F_2, the function R^L does not appear to depend on atomic number A[5].

Therefore the ratio of cross sections is given usually in terms of the ratio of structure functions F_2.

In order to compare our results with the data, where experimentalists already accounted for the difference between proton and neutron, we write the structure function of nucleus as

$$\frac{1}{A}F_{2A}(x, Q^2) = \frac{1}{A}\left(ZF_{2pA} + NF_{2nA}\right) =$$

$$= \frac{F_{2nA}(x, Q^2) + F_{2pA}(x, Q^2)}{2} + \frac{N - Z}{2A}(F_{2nA} - F_{2pA}) \qquad (24)$$

and select the isospin I=0 part of F_2 given by the first term of (24). The ratio which we will discuss reads

$$R_{kin}(x, Q^2) = \frac{F_{2nA}(x, Q^2) + F_{2pA}(x, Q^2)}{F_{2D}(x, Q^2)} \ . \qquad (25)$$

The structure function of the proton in nucleus

$$F_{2pA}(x, Q^2) = \frac{1}{Z}\sum_\lambda^{(p)} \nu_{p\lambda} F_{2p\lambda}(x, Q^2) \ , \qquad (26)$$

where $\nu_{p\lambda}$ is the actual number of protons on the level λ ($\nu_{p\lambda} = 2j + 1$ for the completely ocupied shell). Note that in the experimental data the variable x was calculated assuming the proton momentum p_N equal to the momentum of a free proton at rest, $p_N = (m_N, 0, 0, 0)$. However to single out the precise "kinematics" one must account for the change of the nucleon

structure function (parton distibutions) in medium caused by the change of the Bjorken variable $x = Q^2/2(p \cdot q)$. In other words calculating the momentum fraction x' carried by the quark we need to use the precise four momentum of the nucleon in medium. That is

$$x' = \frac{Q^2}{2(pq)} = \frac{Q^2}{2(p_0 q_0 - \vec{p}\vec{q})} = \frac{mx}{m + \varepsilon_\lambda - \beta pt} , \tag{27}$$

where $\beta = |\vec{q}|/q_0 = (1 + \frac{4m^2x^2}{Q^2})^{1/2}$ and the variable t is the cosine of the angle between $\vec{p}$ and $\vec{q}$.

Next we have to note that the structure function F_2, which at the LO reads

$$F_2 = \sum_f e_f^2(xq_f(x) + x\bar{q}_f(x)) \tag{28}$$

(e_f is the electric charge of the quark of flavour f)
contains two factors: the quark(antiquark) distribution $q(x)(\bar{q}(x))$ and the kinematical factor x. The origin of this kinematical factor is as follows. The covariant quantity is not the cross section but discontinuity of the dimensionless interaction amplitute $ImA \simeq s\sigma$. Going from the amplitude A to the cross section $\sigma \propto 1/Q^2$ we obtain the factor $x_A = Q^2/2(pq)$ which corresponds to the true nucleus target and must be calculated as $x_A = AQ^2/2m_A\nu$, where m_A is the mass of nucleus and $\nu = q_0$ is the photon energy in the nucleus rest frame. Note that in the final expressions (29,30) we use the value of m_A calculated within the doorway formalism, that is $m_A = \sum_\lambda^{(p)} \nu_{p\lambda}(m + \varepsilon_\lambda) + \sum_\lambda^{(n)} \nu_{n\lambda}(m + \varepsilon_\lambda)$, which is about 3% less than the true mass of a nucleus in the ground state[3]. This is equivalent to the prescription given in [4], where the authors accounted for the relativistic flux factor and used the baryon charge conservation to normalize the spectral functions $S_p(\varepsilon, \vec{p})$ and $S_n(\varepsilon, \vec{p})$.

Thus in (26) we need to calculate the function

$$F_{2p\lambda}(x, Q^2) = \frac{1}{2} \int_0^{p_\lambda} f_\lambda(p) p^2 dp \int_{-1}^1 \frac{x_A}{x'} F_{2p}(x', Q^2) dt +$$

---

[3]For example, the 'doorway' mass of ^{40}Ca is $m(doorway) = 0.968m(ground\ state)$

$$+ \frac{1}{2} \int_{p_\lambda}^{\infty} f_\lambda(p) p^2 dp \int_{-1}^{p_\lambda/p} \frac{x_A}{x'} F_{2p}(x', Q^2) dt \ . \qquad (29)$$

Here: $p_\lambda = ((1-x)m + \varepsilon_\lambda)/\beta$, and $f_\lambda(p)$ was defined in sect.2.2 [4]

Exactly the same formulae is used for the neutron in nucleus.
For the deuteron

$$F_{2D}(x, Q^2) = \frac{1}{2} \int_0^{p_D} f_D(p) p^2 dp \int_{-1}^{1} \frac{x_D}{x'_D} (F_{2p}(x'_D, Q^2) + F_{2n}(x'_D, Q^2)) dt +$$

$$+ \frac{1}{2} \int_{p_D}^{\infty} f_D(p) p^2 dp \int_{-1}^{p_D/p} \frac{x_D}{x'_D} (F_{2p}(x'_D, Q^2) + F_{2n}(x'_D, Q^2)) dt \qquad (30)$$

with

$$x'_D = \frac{mx}{m_D - \sqrt{p^2 + m^2} - \beta pt}$$

and $p_D = (\beta(m_D - mx) - \sqrt{(m_D - mx)^2 + (\beta^2 - 1)m^2}\ )/(\beta^2 - 1)$; $f_D(p)$ is just the sum of the squared monopole and quadrupole components of the deuteron wave function; m_D is the deuteron mass. Note that denominator in the expression for x'_D corresponds to the kinematics where the spectator nucleon is on mass-shell.

The $F_{2p}(x, Q^2)$ and $F_{2n}(x, Q^2)$ free nucleon structure functions were calculated using the MRST2002 NLO parametrization [18] obtained from the global parton analysis.

4   Discussion

The results of calculations are presented in Table 1-5 and Fig.1. The predictions made using the Bonn-B and OSBEP potentials are very close to each other. So we present the results for the case of Bonn B potential only.

---

[4] Strictly speaking (29) is correct for a positive p_λ only. When x is close to 1 and p_λ becomes negative one has to keep only the last term in (29) with the integration from $-p_\lambda$ up to ∞. In this case the values of $t < 0$ and $x' < x$. So the quantity $F_{2\lambda}$ has non zero value even at $x = 1$. Note however that for experimentally available x values the quantities p_λ never become negative.

^{12}C		$NA-037$	$NMC[19]$	
x	Q^2	R_{exp}	$(\pm)$	R_{kin}
.125	12.0	1.032	(.012)	0.997
.175	15.0	1.011	(.015)	0.994
.250	20.0	1.010	(.015)	0.990
.350	27.0	0.971	(.020)	0.985
.450	32.0	0.975	(.029)	0.985
.550	37.0	0.925	(.043)	0.999
.650	41.0	0.873	(.064)	1.052

Table 1: The ratio of structure functions F_2^A measured on carbon to that on deuteron. The values of Q^2 are given in GeV^2.

Recall that here we <u>assume</u> the parton distributions inside the nucleon in nucleus to be the same as that for the free nucleon and evaluate the pure kinematical effect of the boundness and the motion of nucleon in nuclear matter. Using the doorway states, which are the correct eigen functions to describe the fast interaction with one nucleon, we account for the full <u>4-momemtum</u> of the (target) nucleon and for the exitation of the "residual" nucleus $(A-1)$.

Thus the difference between the calculated value of R_{kin} and the data indicates the distortion of the parton wave function of a nucleon placed in nuclear medium.

As expected the account of the boundness and Fermi motion of nucleons in nuclei diminishes the cross section in the $x = 0.2 - 0.63$ interval. Indeed, due to the boundness (and the fact that about 24 - 27 MeV is spent for the exitation of the residual $(A-1)$ nucleus) the mean value of shifted argument x' (27) is larger than the value of x on a free nucleon. On the other hand in this domain the free nucleon structure function F_2 falls down with x. Therefore we get $R_{kin} < 1$.

At a large x, close to 1, the details of angular integration (over t in (29)) become important. For a negative t, due to a Fermi motion, there is a region where $x' < x$ (see (27)). Thanks to the contribution coming from this region

^{14}N		$NA-4$	$BCDMS$[20]	
x	Q^2	R_{exp}	$(\pm)$	R_{kin}
.100	32.0	1.018	(.039)	0.997
.140	40.0	1.018	(.031)	0.995
.180	49.0	1.002	(.024)	0.993
.225	56.0	1.035	(.025)	0.990
.275	56.0	1.024	(.027)	0.988
.350	67.0	0.983	(.025)	0.985
.450	77.0	0.941	(.031)	0.985
.550	84.0	0.891	(.047)	0.999
.650	96.0	0.826	(.075)	1.053

Table 2: The ratio of structure functions F_2^A measured on nitrogen to that on deuteron. The values of Q^2 are given in GeV^2.

the value of R_{kin} becomes larger than 1 for $x > 0.65 - 0.7$.

Clearly, besides the Fermi motion there should be some dynamical effects. At a large x the growth of the ratio $R(x, Q^2)$ with x is usually atributed to a short range nucleon-nucleon correlations[25] or to a multiquark bags[26] (see for a details the reviews [5, 25] and reference therein). However, contrary to the conventional expectations, the theoretical value of R_{kin} resulting after account of the Fermi motion in the doorway states is even *larger* than the value R_{exp} measured experimentally[5].

This means that in nuclear medium the (one nucleon) parton distribution becomes softer, that is the probability to find a parton with $x > 0.45$ inside the in-medium-nucleon is less than that in a free nucleon. In other words in medium the quark distribution is shifted towards a lower x, leading to the decrease of quark density at $x > 0.45$ and a larger quark density at a lower $x \sim 0.1 - 0.2$.

Next at small $x < 0.2$ the partons from different (neighbouring) nucleons start to overlap and to interact with each other. Indeed, according to un-

---

[5]Since the same effect was observed both at relatively low Q^2 in SLAC data and for a larger Q^2 at CERN this can not be explained by the account of the mass correction.

^{40}Ca		$NA-037$	$NMC[21]$	
x	Q^2	R_{exp}	$(\pm)$	R_{kin}
.113	4.3	0.994	(.010)	0.998
.138	5.1	1.007	(.012)	0.996
.175	6.2	1.001	(.011)	0.994
.225	7.7	1.015	(.014)	0.990
.275	9.1	0.998	(.018)	0.986
.350	11.0	0.996	(.019)	0.981
.450	14.0	1.024	(.031)	0.978
.600	17.0	0.955	(.038)	1.005

Table 3: The ratio of structure functions F_2^A measured on calcium to that on deuteron. The values of Q^2 are given in GeV^2.

certainty principle the characteristic size of localization is $\Delta r \sim 1/mx$ and for $x < 0.2$ the value of $\Delta r > 1$fm becomes comparable with the nucleon-nucleon separation. At a very low x the partons screen each other and this shadowing correction results in decreasing of $R(x,Q^2)$. Another way to describe this effect is to say that two low-x partons from two different nucleons recombine into one parton. However the whole energy must be conserved. This leads to the antishadowing (growth of the parton density)[27] (see the reviews[5, 25] for more details) just in the region ($x \sim 0.1 - 0.2$) of the begining of recombination. On the other hand this antishadowing effect is expected to reveal itself more in the gluon distributions than in the quark structure function.

Thus it is not surprising that in the interval $0.2 < x < 0.45$ the ratio given by the pure kinematical effects R_{kin} (25)is close (within the error bars) to that observed experimentally R_{exp}.

Note that, at large x, the Fermi motion is not negligible, even for the deuteron. The ratio $R_{D,kin} = F_{2D}/(F_{2p} + F_{2n})$ is close to one for $x < 0.65$, but it noticeably differs from one for $x > 0.75$, reaching values of $R_{D,kin} = 1.07$ (1.42) at $x = 0.75$ (0.85); see Table 6.

An analysis performed by the MRST group shows that if this effect is included then one obtains practically the same partons, but the description

^{56}Fe		$NA-4 \quad BCDMS[22]$		
x	Q^2	R_{exp}	$(\pm)$	R_{kin}
.100	22.0	1.057	(.021)	0.996
.140	25.0	1.046	(.020)	0.994
.180	29.0	1.050	(.018)	0.991
.225	46.0	1.027	(.019)	0.988
.275	49.0	1.000	(.021)	0.984
.350	59.0	0.959	(.020)	0.979
.450	72.0	0.923	(.028)	0.977
.550	72.0	0.917	(.040)	0.991
.650	72.0	0.813	(.053)	1.047

Table 4: The ratio of structure functions F_2^A measured on iron to that on deuteron. The values of Q^2 are given in GeV^2.

of the high x deuteron data is much improved; with χ^2 reduced by 20 for the 12 deuteron data points that are fitted at $x = 0.75$ [6].

After the present work was completed we have read the recent paper of A.Molochkov [28] where a little bit another (but not quite different from that used here) prescripton was proposed to account for the boundness and momentum distribution of nucleons. A.Molochkov had considered the ratio of the ^{4}He to deuteron structure functions. The shortness of his prescription is the assumption that both the nucleon structure function F_2 and the momentum distribution of the nucleons in nucleus $f^N(P_A, p)$ are regular (i.e. have no singularities) with respect to p_0. Besides this some terms, coming from the differentiation of the nucleus $(A-1)$ propagator and the factor $1/(p_0 + \sqrt{m^2 + p^2})^2$ (corresponding to the antinucleon pole) in the nucleon propagator, which are proportional to the binding (or nuclear exitation) energy, were omitted in [28]. We hope that our approach, based on the 'doorway' formalism is more precise. Moreover, in terms of the Molochkov's integral our result may be obtained by closing the integration contour over p_0 in the upper half-plane (on the pole corresponding to the residue $(A-1)$

---

[6]We thank R.S.Thorne and A.D.Martin for discussions and for performing a new analysis using our Fermi motion in the deuteron.
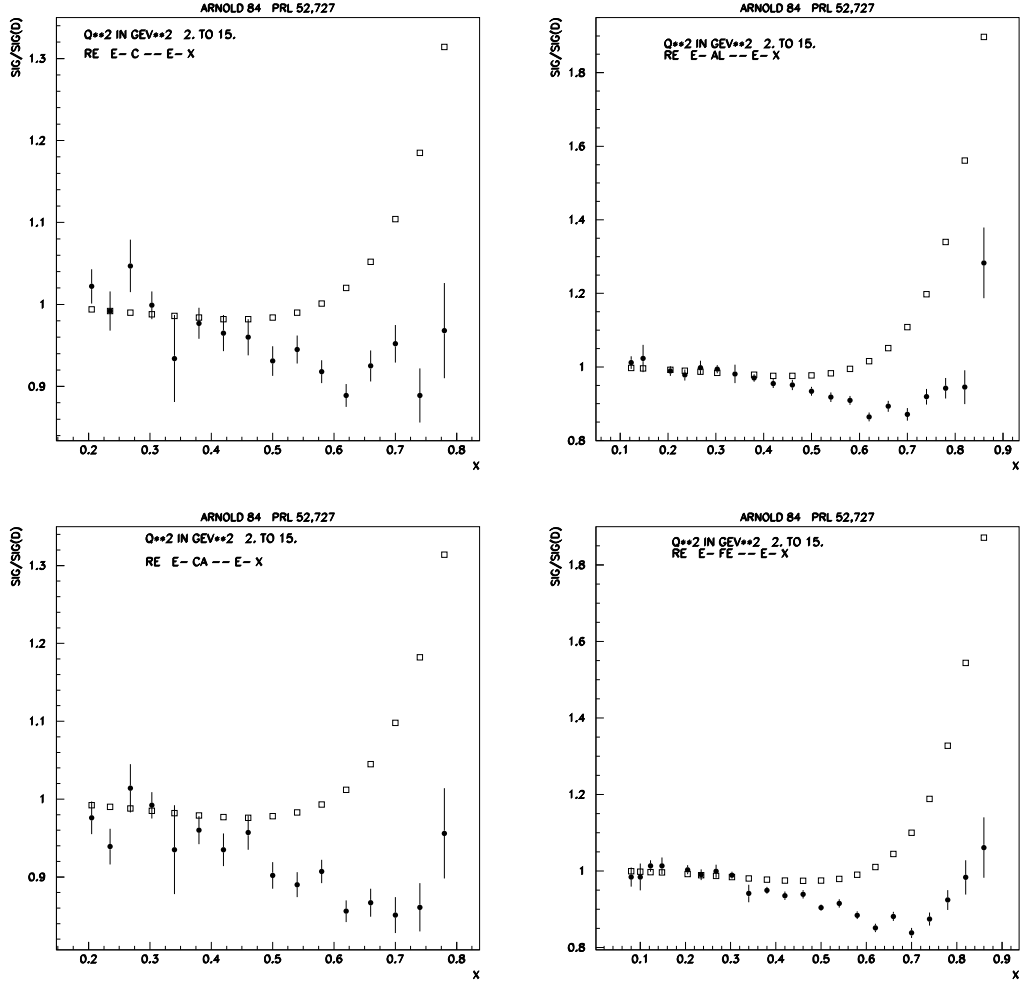
15

Figure 1: Fig.1 The ratio of structure function F_2^A measured on nucleus A to that on deuteron. $Q^2 = 5$ GeV^2. The data are taken from [24]. The empty bar is the ratio R_{kin} calculated using the Bonn-B potential.

^{63}Cu		$NA-037$	NMC[23]	
x	Q^2	R_{exp}	$(\pm)$	R_{kin}
.123	11.0	1.041	(.026)	0.996
.173	16.1	1.031	(.023)	0.993
.243	19.3	1.018	(.024)	0.988
.343	25.8	0.962	(.032)	0.981
.444	36.0	0.959	(.047)	0.978
.612	46.4	0.918	(.056)	1.016

Table 5: The ratio of structure functions F_2^A measured on copper to that on deuteron. The values of Q^2 are given in GeV^2.

nucleus) instead of the lower one as it was done in[28].

However we are planning to compare both approaches in the forthcoming paper, using the doorway eigen functions to describe the distributions of nucleons in a heavier nuclei.

References

[1] J.J.Aubert et al., Phys. Lett. B123 (1983) 275.

[2] A.Bodek and J.L.Ritchie, Phys. Rev. D23 (1981) 1070; D24 (1981) 1400.

[3] S.V.Akulinichev et al., Phys. Rev. Lett. 55 (1985) 2239.

[4] L.Frankfurt and M.Strikman, Phys. Lett. B183 (1987) 254.

[5] M.Arneodo, Phys. Rept. 240 (1994) 301.

[6] S.Frullani and J.Mougey, Adv. Nucl. Phys. 14 (1984) 1.

[7] B.L. Birbrair and V.I. Ryazanov, Yad. Fiz. **63**, 1842 (2000).

[8] B.L. Birbrair and V.I. Ryazanov, Yad. Fiz. **64**, 471 (2001).

[9] B.L. Birbrair and V.I. Ryazanov, Eur. Phys. J. **A15** (2002) 343.

[10] B.L.Birbrair et al., Phys. Lett. B166 (1986) 119.

x	$Q^2 = 5$	10	20	50	100	200	GeV^2
.05	$R_{kin} =$ 1.000	.999	.999	.999	.998	.998	
.10	$R_{kin} =$ .999	.999	.998	.998	.997	.997	
.14	$R_{kin} =$ .998	.998	.997	.997	.996	.996	
.20	$R_{kin} =$ .996	.996	.995	.995	.994	.994	
.35	$R_{kin} =$ .990	.990	.989	.989	.989	.989	
.45	$R_{kin} =$ .987	.987	.987	.987	.987	.987	
.55	$R_{kin} =$ .988	.988	.988	.989	.990	.991	
.65	$R_{kin} =$ 1.005	1.004	1.004	1.006	1.008	1.011	
.75	$R_{kin} =$ 1.080	1.073	1.071	1.075	1.080	1.085	
.85	$R_{kin} =$ 1.440	1.396	1.382	1.391	1.408	1.431	

Table 6: The kinematical part R_{kin} of the ratio $F_2^d/[F_2^p + F_2^n]$ calculated using the Bonn-B potential

[11] A.A. Abrikosov, L.P. Gor'kov, and I.E. Dzyaloshinsky, *"Methods of quantum field theory in statistical physics"* Prentice-Hall, Englewood Cliffs, 1963.

[12] A.B. Migdal, *"Theory of finite Fermi-systems and applications to atomic nuclei"*, Nauka, M. 1983.

[13] R.Machleidt, K.Holinde and Ch.Elster, Phys. Rept. 149 (1987) 1.

[14] H. de Vries et al., At. Data and Nucl. Data Tables 36 (1987) 495.

[15] G.D.Alkhazov et al., Nucl. Phys. A381 (1982) 430.

[16] G.D.Alkhazov, private communication.

[17] L.Jäde and H.V. von Geramb, Phys. Rev. C57 (1998) 496.

[18] A.D.Martin, R.G.Roberts, W.J.Stirling and R.S.Thorne, Eur. Phys. J. C28 (2003) 455.

[19] M.Arneodo at al. Nucl. Phys. B441 (1995) 12.

[20] G.Bari at al. Phys. Lett. 163B (1985) 282.

[21] P.Amadruz at al. Nucl. Phys. B441 (1995) 3.

[22] A.C.Benvenuti et al. Phys. Lett. 189B (1987) 483.

[23] J.Ashman at al. Zeit. Phys. C57 (1993) 211.

[24] R.G.Arnold et al. Phys. Rev. Lett. 52 (1984) 727.

[25] L.L.Frankfurt and M.I.Strikman, Phys. Rept. 160 (1988) 235.

[26] R.L.Jaffe Phys. Rev. Lett. 50 (1983) 228;
C.E.Carlson and T.J.Havens, Phys. Rev. Lett. 51 (1983) 261;
S.Date and A.Nakamura, Prog. Theor. Phys. 69 (1983) 565;
H.Faissner and B.B.Kim, Phys. Lett. B130 (1983) 321;
H.J.Pirner and J.P.Vary, Phys. Rev. Lett. 46 (1981) 1376, Nucl. Phys.
A358 (1981) 413c.

[27] N.N.Nikolaev and V.I.Zakharov,
Yad. Fiz. 21 (1975) 434; Sov.J.Nucl.Phys. 21 (1975) 227; Phys. Lett.
B55 (1975) 397; Z.Phys. C49 (1991) 607.

[28] A.Molockov, arXiv:nucl-th/0407077